RNA (2000), *6*:511–519. Cambridge University Press. Printed in the USA.

REPORT

Helix P4 is a divalent metal ion binding site in the conserved core of the ribonuclease P ribozyme

ERIC L. CHRISTIAN, NICHOLAS M. KAYE, and MICHAEL E. HARRIS

Center for RNA Molecular Biology, Department of Molecular Biology and Microbiology, Case Western Reserve University School of Medicine, Cleveland, Ohio 44106, USA

ABSTRACT

The ribonuclease P ribozyme (RNase P RNA), like other large ribozymes, requires magnesium ions for folding and catalytic function; however, specific sites of metal ion coordination in RNase P RNA are not well defined. To identify and characterize individual nucleotide functional groups in the RNase P ribozyme that participate in catalytic function, we employed self-cleaving ribozyme–substrate conjugates that facilitate measurement of the effects of individual functional group modifications. The self-cleavage rates and pH dependence of two different ribozyme–substrate conjugates were determined and found to be similar to the single turnover kinetics of the native ribozyme. Using site-specific phosphorothioate substitutions, we provide evidence for metal ion coordination at the *pro*-R_P phosphate oxygen of A67, in the highly conserved helix P4, that was previously suggested by modification-interference experiments. In addition, we detect a new metal ion coordination site at the *pro*-S_P phosphate oxygen of A67. These findings, in combination with the proximity of A67 to the pre-tRNA cleavage site, support the conclusion that an important role of helix P4 in the RNase P ribozyme is to position divalent metal ions that are required for catalysis.

Keywords: metal ion coordination; phosphorothioate; ribozyme; RNase P RNA

INTRODUCTION

Like many protein enzymes, large ribozymes (group I and group II introns and ribonuclease P [RNase P]) utilize magnesium ions to catalyze transesterification and phosphodiester bond hydrolysis (Pyle, 1996). For both RNA and protein enzymes, the ability of divalent metal ions, other than magnesium, to rescue the deleterious effects of phosphorothioate modifications provides a biochemical signature for metal ion interactions with phosphate oxygens (Knowles, 1980; Eckstein, 1985; Narlikar & Hershlag, 1997). This approach, combined with analysis of the reaction kinetics of modified RNAs, has been particularly useful for elucidating how magnesium ions are coordinated to substrate phosphates in ribozyme-catalyzed reactions (e.g., Piccirilli et al., 1993; Warnecke et al., 1996; Weinstein et al., 1997; Scott & Uhlenbeck, 1999; Shan et al., 1999; Yoshida et al., 1999). In contrast to the detailed perspective on interactions of metal ions at scissile phosphates, less is known about the coordination of essential divalent metal ions within the catalytic centers of the large ribozymes themselves.

Ribonuclease P is a widespread and essential ribonucleoprotein endonuclease that generates the mature tRNA 5′ end during tRNA maturation (for reviews, see Frank & Pace, 1998; Altman & Kirsebom, 1999). The RNA subunits from many bacterial RNase P enzymes are catalytic, and can bind to pre-tRNA and catalyze hydrolysis at the appropriate phosphodiester bond in the absence of protein in vitro, and so comprise one class of large ribozymes (Guerrier-Takada et al., 1983). Optimal substrate binding in vitro requires a small RNase P-associated protein or elevated concentrations of monovalent ions (Reich et al., 1988; Kurz et al., 1998). However, the RNase P ribozyme, whether in the presence or absence of its associated protein, requires millimolar concentrations of magnesium to catalyze phosphodiester bond hydrolysis (Guerrier-Takada et al., 1986; Smith et al., 1992; Beebe et al., 1996).

Like group I and group II introns, the RNase P ribozyme has a dual requirement for magnesium ions. Magnesium is essential for folding into the active conformation (Pan, 1995; Zarrinkar et al., 1996; Pan & Sosnick, 1997), and is also likely to participate directly in catalysis (Guerrier-Takada et al., 1986; Smith & Pace,

Reprint requests to: Michael E. Harris, Department of Molecular Biology and Microbiology, Case Western Reserve University School of Medicine, Cleveland, Ohio 44106, USA; e-mail: meh2@po.cwru.edu.

1993; Beebe et al., 1996; Warnecke et al., 1996). The general folding pathway of the ribozyme has been outlined (Pan & Sosnick, 1997; Pan et al., 1999) and the requirement for magnesium ions in this process defined; however, specific magnesium binding sites within the ribozyme are not well understood. Similarly, functional groups within the ribozyme that direct folding or form the ribozymes active site are only just coming into focus.

The RNase P ribozyme is composed of two domains that can fold independently (Pan, 1995; Loria & Pan, 1996). The S-, or specificity, domain is composed of helices P7–P14 and contacts the T-stem of the pre-tRNA substrate, as demonstrated by kinetic (Pan et al., 1995; Loria & Pan, 1998) and photocrosslinking studies (Nolan et al., 1993; Chen et al., 1998). The C-, or catalytic, domain is composed of helices P1–6 and P15–18, and contains the majority of nucleotide positions that are conserved among all known RNase P RNAs (Chen & Pace, 1997). The C-domain forms efficient photocrosslinks to photoagents positioned at the pre-tRNA cleavage site (Burgin & Pace, 1990; Kufel & Kirsebom, 1996; Christian & Harris, 1999). In addition, the binding site for the substrate 3′ CCA sequence is located in a region of non-Watson–Crick base pairing included in the C-domain (Kirsebom & Svard, 1994). Also, the C-domain alone can catalyze the cleavage of RNA substrates selected in vitro (Pan & Jakacka, 1996). Taken together these results demonstrate that the C-domain contains the active site of the native ribozyme. However, the individual chemical groups that comprise the active site and the roles they play are not yet defined.

Helix P4, located in the C-domain of the ribozyme, has been suggested to contain functional groups and sites of metal ion coordination central to ribozyme activity. This suggestion is based in part on phylogenetic comparative analysis of RNase P RNA sequences that demonstrated that nucleotides in helix P4, and adjoining single-stranded regions, are universally conserved in bacterial, archeal, and eukaryal RNase P RNAs (Chen & Pace, 1997). In addition, nucleotide analog interference experiments identified functional groups in P4 that are important for both substrate binding and catalysis (Hardt et al., 1995, 1996; Harris & Pace, 1995; Kazantsev & Pace, 1998; Heide et al., 1999; Siew et al., 1999). Preliminary evidence for thiophilic metal ion rescue of phosphorothioate effects in P4 (Hardt et al., 1995; Harris & Pace, 1995) and P15 (Kufel & Kirsebom, 1998) have been reported. However, the high concentrations of thiophilic metal ions used in these experiments or the lack of a quantitative assessment of the effects makes a definitive interpretation difficult.

To examine more closely the role of nonbridging phosphate oxygens in helix P4, we measured the effects of site-specific phosphorothioate substitution, focusing on positions that displayed large modification-interference effects on the cleavage reaction (Harris & Pace, 1995). In addition, we examined the effect of sulfur substitution of the corresponding *pro*-S_P nonbridging phosphate oxygens that are not generally analyzed by conventional modification-interference. These studies provide, for the first time, a quantitative assessment of phosphorothioate interference effects in the universally conserved core of the RNase P ribozyme. Importantly, we report confirmation of one previously suggested position of metal ion coordination and evidence for a new site of metal ion coordination with a substantially larger thiophilic metal rescue of the phosphorothioate-induced defect on catalysis. The current work, taken together with available biochemical and phylogenetic information, provides direct evidence that helix P4 is an important divalent metal ion binding site in the conserved core of the RNase P ribozyme.

RESULTS AND DISCUSSION

In the current analysis, the use of two different self-cleaving ribozyme constructs [PT50 and PT332(-5)], facilitated site-specific functional group modifications in helix P4 (Fig. 1). These self-cleaving constructs allow site-specific functional group modifications to be introduced into the conserved core of the ribozyme by ligation of short synthetic oligonucleotides (Moore & Sharp, 1992). Importantly, these reagents make possible the kinetic characterization of modified ribozymes that, in a number of cases, could not be obtained in sufficient quantities to be analyzed under standard single-turnover conditions. PT50 and PT332(-5) contain tRNA sequences appended to circularly permuted RNase P RNAs. The design of PT50 and PT332(-5) is based on structural analyses demonstrating that nucleotide −10 in the pre-tRNA 5′ leader sequence is adjacent to helix P3 (Christian & Harris, 1999), and that positions −2 to −5 in the pre-tRNA 5′ leader sequence are adjacent to J18/2 of the RNase P ribozyme (Burgin & Pace, 1990). Modifications to the 5′ half of helix P4 were introduced into PT50, whereas those adjacent to the 3′ half of helix P4 were incorporated into PT332(-5).

Effective interpretation of site-specific functional group modification effects on ribozyme catalysis requires an understanding of the reaction kinetics of the RNA under investigation. We therefore defined reaction conditions (25 mM Mg^{2+}, 50 mM PIPES, 3 M NaCl, 0.1 mM EDTA, pH 5.5, 50 °C) under which the PT50 and PT332(-5) self-cleavage reactions reflect the single-turnover kinetic behavior of the native ribozyme. PT332(-5) was previously shown to accurately cleave the tethered pre-tRNA substrate (Frank et al., 1994). Similarly, intramolecular cleavage of PT50 generates two products: a small fragment with mobility on denaturing gels similar to mature tRNA, and a larger fragment with mobility of RNase P RNA (Fig. 2A). The reaction of PT50 is thus consistent with a single endo-

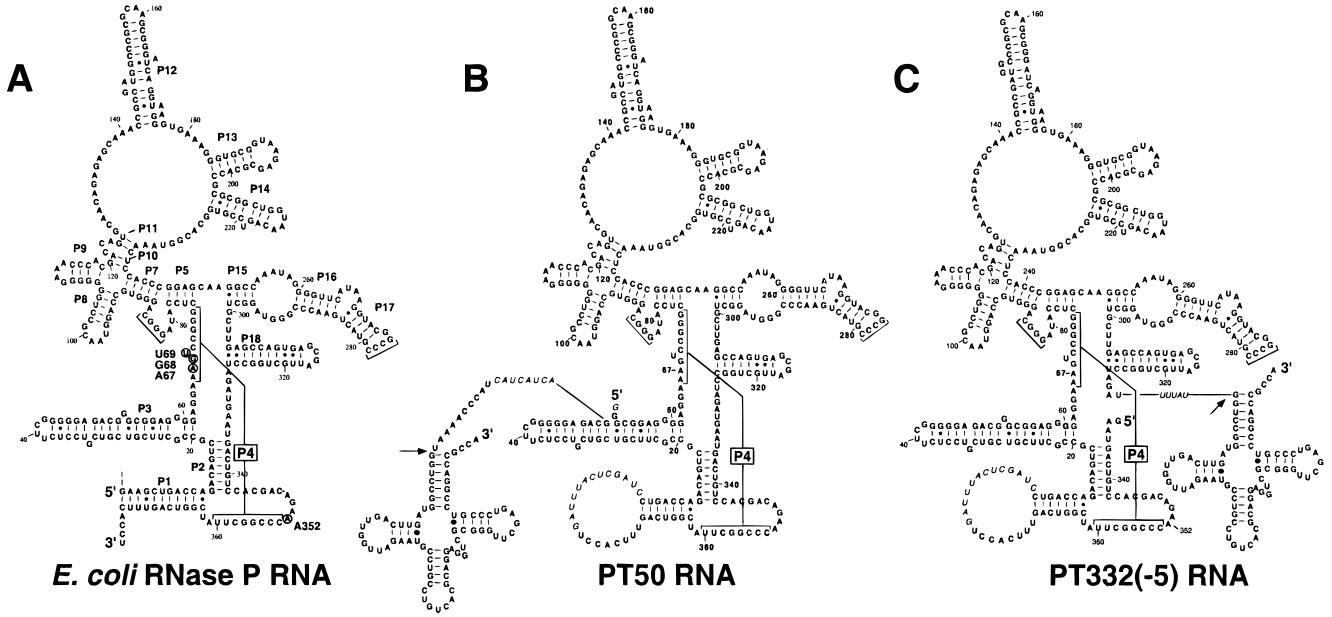

FIGURE 1. Secondary structures of native *Escherichia coli* RNase P RNA, PT50, and PT332(-5). **A**: Native RNase P RNA from *E. coli.* Nomenclature is as described in Haas et al. (1994). Helices are designated as P (paired) and numbered from the 5′ end. Regions between helices are designated as J (joining) and numbered based on the helical elements that they connect. 5′ and 3′ strands of helix P4 are marked by brackets. Nucleotide positions with strong phosphorothioate effects are indicated. **B**: Secondary structure of the PT50 ribozyme. Nonnative sequences are shown in italics and the location of the cleavage site is indicated with an arrow. **C**: Secondary structure of the PT332(-5) ribozyme. The structure is labeled as in **B**.

nucleolytic cleavage at the pre-tRNA cleavage site. To establish the accuracy of PT50 cleavage, a radiolabeled DNA oligonucleotide complementary to the last 20 nt of the tRNA product was annealed to the 3′ cleavage fragment. Hybrids were extended by reverse transcriptase, and the extension products were compared to dideoxy sequencing standards derived from primer extension of the uncleaved RNA (Fig. 2B). The run-off primer extension product corresponded in size to that expected for the mature tRNA 5′ end, demonstrating that PT50 cleavage occurred at the authentic cleavage site.

A time course of product formation demonstrates that the PT50 and PT332(-5) cleavage reactions are described by a single exponential function (Fig. 2C). The observed pseudo-first-order rate constant for cleavage (k_{obs}) of both tethered constructs are similar to each other [0.74 min^{-1} for PT50 and 0.73 min^{-1} for PT332(-5)], and to that catalyzed by native RNase P RNA (0.86 min^{-1}). The observed rate constants for PT50 and PT332(-5) reactions are also insensitive to dilution over a broad range of RNA concentrations (0.02–20 nM), indicating that the reactions are genuinely intramolecular in nature (Frank et al., 1994; data not shown). It was shown previously that a plot of log k_{obs} for the native enzyme versus pH is linear between pH 5.5 and pH 7.5 with a slope near one (Smith & Pace, 1993), suggesting that the reaction rate is limited by hydroxide-ion concentration, and that k_{obs} reflects phosphodiester bond hydrolysis. Although the rate of PT332(-5) self-cleavage is known to be sensitive to pH (Kazantsev & Pace, 1998), the precise pH dependence of the reaction was not determined. Importantly, we find that log k_{obs} for both PT332(-5) and PT50 cleavage are also linearly dependent on pH, with slopes similar to that of the native ribozyme (0.88 for PT332(-5) and 0.81 for PT50; Fig. 2D). PT332(-5) and PT50 thus appear to be useful and accurate tools for analysis of native RNase P RNA catalysis.

Using PT50 and PT332(-5) we incorporated site-specific phosphorothioate substitutions at, and adjacent to, positions with dominant phosphorothioate modification-interference effects (Harris & Pace, 1995), reasoning that these functional groups were more likely to play a direct role in the hydrolysis reaction. These substitutions are located in, or adjacent to, the 5′ (A65 to U69) or 3′ (A352) strands of helix P4 (Fig. 1A), and their effects on ribozyme catalysis are shown in Table 1. The strongest inhibitory effects from *pro*-R_P phosphate oxygen substitutions were observed at A67 and G68, where phosphorothioate modifications resulted in 10,000- and 4,000-fold decreases in k_{obs}, respectively. At A352 and U69 there were comparatively smaller, but significant, decreases of 1,500- and 7-fold upon sulfur substitution of the *pro*-R_P nonbridging phosphate oxygens. In addition, we identified two S_P phosphorothioate sensitive positions (Table 1). S_P phosphorothioate modification at A67 and G68 resulted in 4,000- and 33-fold decreases in k_{obs}, whereas no significant effect was observed at A352 or U69. Little (less than three-

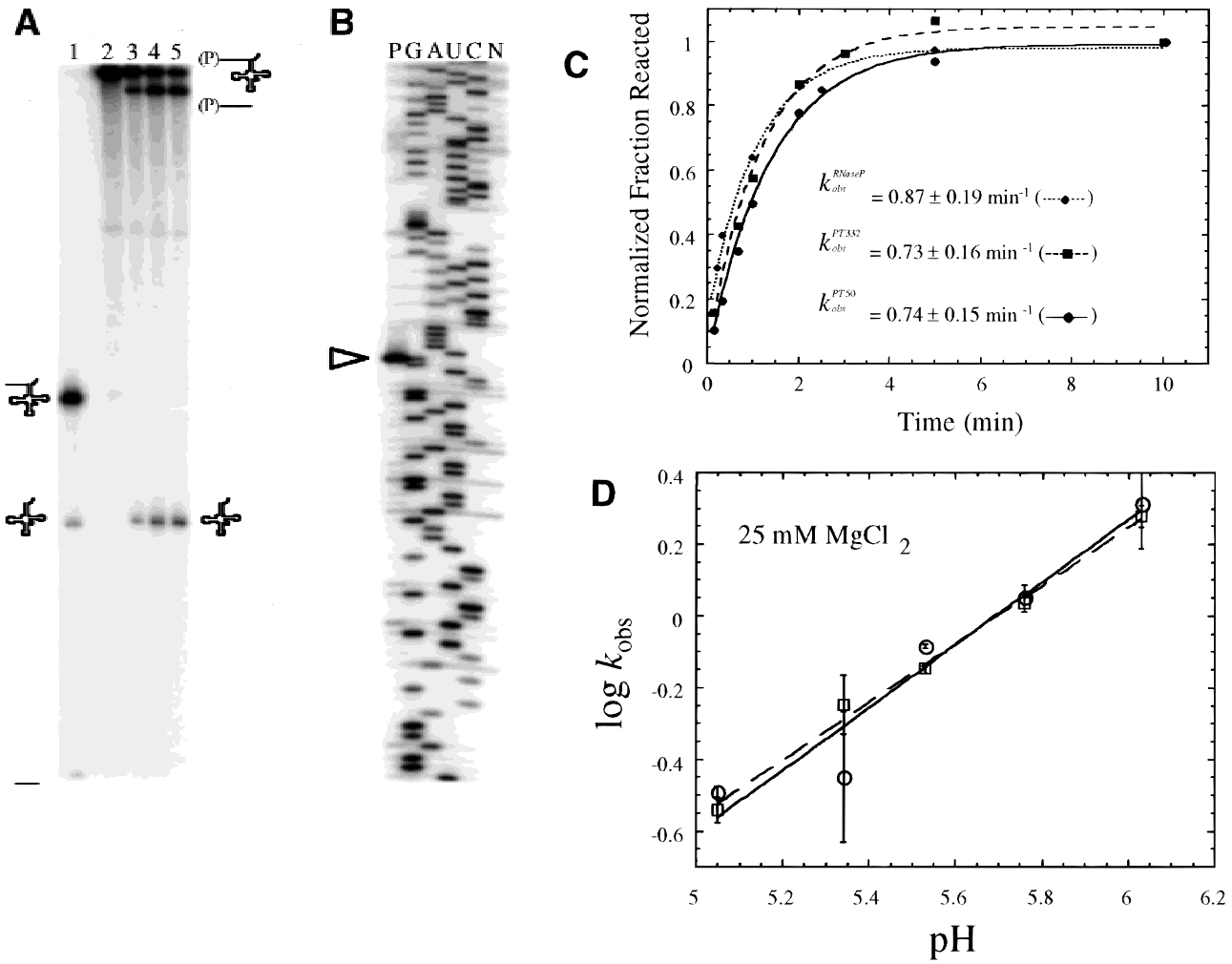

FIGURE 2. Characterization of the PT50 and PT332(-5) self-cleavage reactions. **A**: Comparison of pre-tRNA and PT50 cleavage products. Lane 1 shows a control RNase P ribozyme reaction containing uniformly labeled substrate pre-tRNA. The locations of pre-tRNA, the mature tRNA, and 5′ leader are shown at left. Lanes 2–5 contain the products of reactions containing uniformly labeled PT50 RNA. Lane 2: PT50 RNA incubated in the absence of magnesium. Lanes 3–5: PT50 RNA incubated in the presence of 25 mM $MgCl_2$, 3 M NaCl, 40 mM PIPES, pH 6.0, 0.05% NP-40 at 50 °C for 5, 30, and 600 s, respectively. Positions of PT50 RNA and the products of the self-cleavage reaction are shown at right. **B**: Primer extension mapping of the PT50 cleavage site. The products of a PT50 cleavage reaction and unreacted PT50 RNAs were used as templates for reverse transcriptase primer extension using a primer that anneals to pre-tRNA sequences. Control extension reactions containing dideoxynucleotides were loaded in lanes G, A, U, and C. A control extension reaction that did not contain dideoxynucleotides was loaded in lane N. The extension products from a reaction containing the products from a PT50 cleavage reaction were loaded in the lane marked P. **C**: Reaction time course for *E. coli* RNase P, PT50, and PT332. Ratio of reacted pre-$tRNA^{ASP}$ (cleaved by *E. coli* RNase P, diamonds), PT50 (circles) and PT332(-5) (squares) plotted as a function of time at pH 5.5. A fit of the data to a single exponential function, as described in Materials and Methods, is shown as a dotted line for pre-$tRNA^{ASP}$ cleavage by *E. coli* RNase P, a solid line for the PT50 reaction, and as a dashed line for the PT332(-5) reaction **D**: pH dependence of self-cleaving ribozymes. k_{obs} values for PT50 (squares) and PT332(-5) (circles).

fold) or no effect on k_{obs} was observed for R_P and S_P phosphorothioate modifications at nucleotides A65 and A66, consistent with previous modification-interference studies (Hardt et al., 1995; Harris & Pace, 1995; Table 1). The large phosphorothioate effects observed in this analysis are of the same order of magnitude as those observed at the scissile phosphates of the hammerhead ribozyme (Scott & Uhlenbeck, 1999), group I introns (Piccirilli et al., 1993; Weinstein et al., 1997), and the pre-tRNA substrate of RNase P RNA (Warnecke et al., 1996), and thus are consistent with perturbation of functional groups that may be directly involved in catalytic function.

To determine whether a metal ion binding site was disrupted by phosphorothioate modification in P4, we introduced manganese into reactions to a final concentration of 5 mM along with 20 mM magnesium, to maintain a constant concentration (25 mM) of divalent metal ion. Although most of the positions tested showed less than a threefold increase in k_{obs} due to the presence of

TABLE 1. Effects of phosphorothioate substitutions on RNase P ribozyme catalysis.

Ribosyme	k_{obs}(Mg)	$k_{native}/k_{modified}$	k_{obs}(Mn)	k_{obs}(Mn)/k_{obs}(Mg)	k_{obs}(Cd)	k_{obs}(Cd)/k_{obs}(Mg)
PT50	2.0 ± 0.9	1.0	3.7 ± 0.6	1.8	2.1 ± 0.8	1.0
A65 Rp	1.5 ± 0.1	1.3	1.8 ± 0.2	1.2	nd	nd
A65 Sp	1.3 ± 0.2	1.5	1.9 ± 0.2	1.5	nd	nd
A66 Rp	1.1 ± 0.2	1.8	2.7 ± 1.0	2.7	nd	nd
A66 Sp	1.6 ± 0.4	1.3	3.5 ± 0.4	2.2	nd	nd
A67 Rp	0.00020 ± 0.00009	10000	0.013 ± 0.005	65	0.00093 ± 0.00011	4.7
A67 Sp	0.0005 ± 0.0003	4000	2.6 ± 1.8	5200	0.11 ± 0.02	220
G68 Rp	0.0005 ± 0.0003	4000	0.0008 ± 0.0007	1.6	0.0011 ± 0.0006	2.2
G68 Sp	0.06 ± 0.04	33	0.08 ± 0.04	1.3	0.03 ± 0.02	0.5
U69 Rp	0.3 ± 0.1	6.7	0.7 ± 0.4	2.3	nd	nd
U69 Sp	2.5 ± 1.2	0.8	4.8 ± 0.4	1.9	nd	nd
PT332(-5)	1.7 ± 0.7	1.2	2.6 ± 0.2	1.5	nd	nd
A352 Rp	0.0013 ± 0.0006	1500	0.0016 ± 0.0001	1.2	nd	nd
A352 Sp	2.2 ± 0.5	0.9	2.4 ± 2.1	1.1	nd	nd

Units for k_{obs} are min^{-1}. Errors are one standard deviation determined from the average of at least three measurements. nd indicates not determined. k_{obs}(Mg) indicates the reaction rate constant measured in 25 mM $MgCl_2$, $k_{native}/k_{modified}$ indicates the fold change in reaction rate constant in the presence of $MgCl_2$ and a phosphorothioate substitution. k_{obs}(Mn) indicates the reaction rate constant measured in 20 mM $MgCl_2$ and 5 mM $MnCl_2$, and k_{obs}(Cd) indicates the reaction rate constant measured in 20 mM $MgCl_2$ and 5 mM $CdCl_2$. k_{obs}(Mn)/k_{obs}(Mg) is the fold change in reaction rate constant in the presence of Mn, and k_{obs}(Cd)/k_{obs}(Mg) is the fold change in reaction rate constant in the presence of Cd.

manganese, significant rescue (65-fold) of the effect of phosphorothioate modification was observed at the *pro*-R_P position of A67, confirming the partial rescue observed at this position in modification-interference experiments. Surprisingly, we find a dramatic (5,200-fold) rescue of the newly identified S_P phosphorothioate effect at A67 (Table 1). Notably, under these conditions the rescued rate constant is within experimental error of the unmodified control, and is thus complete. To confirm these effects in the presence of a second thiophilic metal ion, we also examined phosphorothioate rescue in the presence of cadmium. Again, little if any effect is observed with cadmium on the unmodified control, but significant rescue of k_{obs} was found in ribozymes modified at A67 (Table 1). The metal ion rescue effects that we observe do not appear to be due to indirect stabilization of ribozyme structure by manganese or cadmium, as the changes in rate constants of the phosphorothioate-modified RNAs are much larger than that in the unmodified controls. Taken together, these findings indicate a biochemical signature for coordination of divalent metal ion(s) at A67.

An intriguing difference in the metal ion rescue results reported here compared to analyses in other systems is that both the R_P and S_P phosphorothioate modifications at the same phosphate give rise to metal ion rescues. One possibility for these effects is that two different metal ions are coordinated to the two nonbridging phosphate oxygens of A67. An example of metal ions coordinated to both nonbridging oxygens at the same phosphate is found in an A-rich bulge in the P4–P6 domain of the group I intron from *Tetrahymena* (Cate et al., 1997). Alternatively, the thiophilic metal rescue effects seen at A67 could be induced. That is, a thiophilic metal ion is "recruited" to A67 when a sulfur atom is incorporated. Although this explanation may account for the partial rescue of the R_P phosphorothioate modification at A67, it is less likely to account for the large and complete rescue of activity we have identified at the *pro*-S_P phosphate oxygen of A67. It is important to note that the absence of a thiophilic metal ion rescue does not exclude metal ion binding at the other positions where we observe phosphorothioate effects, as disruption of metal ion binding by phosphorothioate modification is not always ameliorated by inclusion of thiophilic metal ions (e.g., Basu & Strobel, 1999; Brautigam & Steitz, 1998).

Interestingly, the site(s) of metal ion binding observed here are adjacent to the pre-tRNA substrate phosphate in the current three-dimensional models of the RNase P ribozyme–substrate complex (Chen et al., 1998; Massire et al., 1998). These models are based on a large collection of phylogenetic comparative and inter- and intramolecular crosslinking data that are sufficient to position the sites of divalent metal ion binding observed here within 10–15 Å (approximately the resolution of the models themselves) of the pre-tRNA cleavage site (Fig. 3C). The positions of metal ion coordination identified here thus appear to be adjacent to functional groups shown to be involved in metal ion binding at the scissile phosphate (Warnecke et al., 1996; Chen et al., 1997).

Consistent with a direct involvement of P4 in catalysis, the strong phosphorothioate effects we observe are adjacent to nucleotides conserved in all three phylogenetic kingdoms (Chen & Pace, 1997; Fig. 3A) and are on the same helical face across the major groove of the P4 helix (Harris & Pace, 1995; Fig. 3B). Struc-

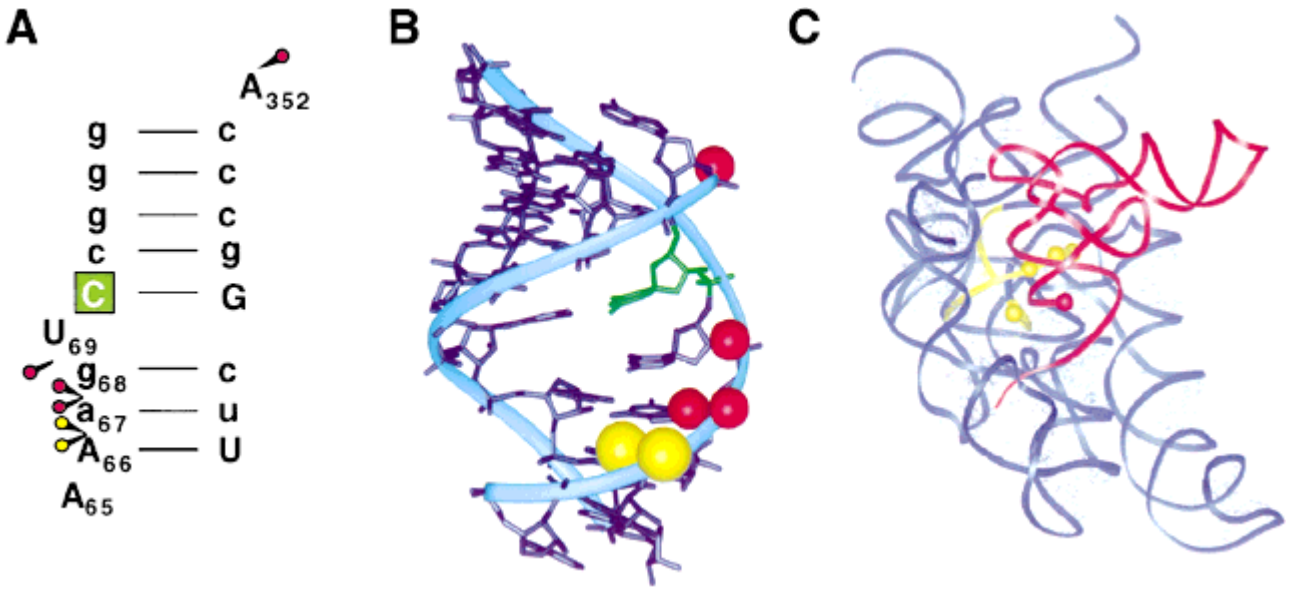

FIGURE 3. Position of phosphorothioate effects on structural models the *E. coli* RNase P ribozyme. **A**: Position of phosphorothioate effects on the secondary structure of helix P4. Universally conserved nucleotides are in upper case. Position C70 is boxed. Phosphorothioate-sensitive positions discussed in the text are shown as colored circles. Yellow circles indicate positions in which the inhibitory effect of phosphorothioate substitution could be rescued in the presence of thiophilic metal ions and red positions indicate positions that could not. **B**: A-form model of helix P4. Phosphorothioate-sensitive positions are labeled as in **A**. Position C70 is shown in green. **C**: Location of P4 and associated metal binding sites in a model of the RNase ribozyme–substrate complex. The model presented is from Chen et al. (1998). tRNA sequences are shown as a red ribbon. Only the backbone of tRNA is shown for clarity. The RNase P cleavage site at the 5′ end of tRNA is shown as a red sphere. RNase P sequences are shown in blue, except for helix P4, which is shown in yellow. The phosphorothioate-sensitive positions discussed in the text are shown as yellow spheres.

tural analyses of divalent metal ion binding sites in RNA indicates that the major groove is a common site for magnesium ion coordination (e.g., Cate & Doudna, 1996; Correll et al., 1997), and it is clear that helix junctions and noncanonical base pairs can alter helical geometry sufficiently to allow interactions in the relatively deep and inaccessible major groove of A-form helices (Weeks & Crothers, 1993; Patel, 1999). Major groove recognition is clearly important for binding the guanosine cofactor during group I intron self-splicing (Michel et al., 1989), and Pyle and coworkers have proposed that the major groove of the conserved domain V of group II intron ribozymes may function directly in catalysis (Konforti et al., 1998). Interestingly, in helix P4 the site(s) of metal ion binding are adjacent to position C70, where a C-to-U mutation results in a dramatic increase in the utilization of calcium as a catalytic metal ion (Frank & Pace, 1997), indicating that the geometry of functional groups within this region of the ribozyme is particularly important for utilization of metal ions for catalysis. Thus, in the context of available biochemical and phylogenetic information, the evidence presented here demonstrates that helix P4 is an important divalent metal ion binding site in the catalytic core of the RNase P ribozyme, and may comprise a portion of the active site itself.

MATERIALS AND METHODS

Plasmid construction and RNA synthesis

Plasmids pPT332(-5) and pPT50 were derived from plasmid pTAN (Nolan et al., 1993). Plasmid pPT332(-5) was generously supplied by the laboratory of Dr. Norman Pace. Plasmid pPT50 was synthesized from two separate rounds of polymerase chain reaction (PCR) (Sarkar & Sommer, 1990). Specifically, the tRNA portion of PT50 was generated using PCR with primer PT50F (5′-CTCTTCGGGGGAGACGACTAC TACTACCCAAAATGGTCCGGTAG-3′) and primer PT30CP3′ (5′-CGGGATCCGAAGACAGTGGCGGTCCGGACGGGAC TC-3′) and plasmid pDW152 (also supplied by Dr. Norman Pace) as the target DNA. The circularly permuted RNase P RNA portion of the ribozyme was similarly generated using the primers PT50R (5′-CGTCTCCCCCGAAGAG-3′) and PT30CPF (5′-GGAATTCTAATACGACTCACTATAGGGCGG AGGGGAGGAAAGTCCG-3′). PCR products were gel purified on 2% agarose (TBE) gels. The full-length PT50 ribozyme was subsequently synthesized by taking advantage of the regions of complementarity between the tRNA and RNase P PCR products in a second round of PCR amplification. pG73PT50 (see below) was generated from pPT50 by a single round of PCR using primers GAP73PT50 (5′-GGAATT CTAATACGACTCACTATAGGCTCCATAGGGCAGGGUGC-3′) and PT30CP3′ under the conditions above. Similarly, pG364PT332 (see below) was generated from pPT332(-5)

by a single round of PCR using primers GAP364PT33 (5′-GGAATTCTAATACGACTCACTATAGGTCAGTTTCACCTGATTTA-3′) and PT30CP3′. PT50, PT332(-5), G73PT50, and G364PT332 PCR products were digested with *Eco*R1 and *Bam*H1 (New England Biolabs) to generate ends suitable for ligation into pUC18.

Uniformly labeled RNA was synthesized by in vitro transcription of linearized plasmids [plasmids were digested with *Bbs*I for pPT50, *Fok*I for pPT332(-5), and *Bst*N1 for pDW152] by T7 RNA polymerase (80 U) in 40 mM Tris-HCl (pH 7.9), 6 mM $MgCl_2$, 2 mM spermidine, 10 mM DTT (polymerase and buffer provided by Ambion), 1 mM rATP, rCTP, and rUTP, 0.4 mM rGTP, 100 μCi [α^{32}P] GTP at 37 °C for 6 h. To generate RNAs suitable for 5′-end labeling or ligation [e.g., G73PT50 and G364PT332(-5)], transcription conditions were as described except guanosine was added to 6 mM and rNTP levels were increased to 1 mM. RNAs were subsequently ethanol precipitated, resuspended in 10 μL 1 mM EDTA and 10 μL of loading buffer (98% Formamide, 10 mM EDTA, pH 8.0, 0.025% xylene cyanol FF, 0.025% bromophenol blue), heated to 90 °C for 2 min and purified on a 6% (19:1) polyacrylamide (8 M urea) gel. Labeled RNAs were visualized by autoradiography and unlabeled RNAs were visualized by UV shadowing. RNA transcripts were excised from the gel and eluted in a 5–10-fold volume excess (800 μL) of elution buffer (40 mM Tris-HCl, pH 7.5, 1 mM EDTA, 0.3 M sodium acetate, and 0.1% sodium dodecyl sulfate) for 4–12 h. Eluted products were extracted twice with an equal volume of a 1:1 mixture of phenol and chloroform, extracted once with an equal volume of chloroform and then precipitated with three volumes of ethanol. The 5′ ends of G73PT50 and G364PT332 RNAs were subsequently phosphorylated with T4 polynucleotide kinase (Gibco-BRL) and ATP, and gel purified as described above prior to use.

PT50 and PT332 cleavage reactions

Although experimental conditions were varied with respect to metal ion concentration and pH, standard reactions were performed in the following manner. Six microliters of transcribed or ligated RNA (2 nM) dissolved in 1 mM EDTA (and 0.1% NP-40 for ligated RNAs) were mixed with 48 μL of reaction buffer (3.75 M NaCl, 62.5 mM PIPES, pH 5.5 at 50 °C) and annealed in a PTC-100 programmable thermal controller (MJ Research; 85 °C for 1 min, cooled to 65 °C at 0.2 °C per second, maintained at 65 °C for 5 min, cooled to 50 °C at 0.25 °C per second and incubated for 3.5 h at 50 °C). Reactions were then initiated by adding 6 μL 250 mM $MgCl_2$. The final reaction conditions were 0.2 nM RNA, 25 mM $MgCl_2$, 3 M NaCl, 50 mM PIPES, pH 5.5, 50 °C. $MgCl_2$ was mixed into the solution by rapid pipetting for 5 s. For high-pH or high-$MgCl_2$ experiments, mixing typically lasted 2 s. Six microliter aliquots were removed at various times and quenched by mixing with formamide gel-loading buffer containing a 2:1 excess of EDTA relative to $MgCl_2$ (typically 10 mM EDTA, 98% formamide). Products were loaded directly onto 6% polyacrylamide (8 M urea) gels and the products visualized by phosphorimage analysis (Molecular Dynamics). Experiments where metal concentrations were varied were performed as described above, but with corresponding changes in the concentration of $MgCl_2$ and $MnCl_2$ used to start the reaction. Similarly, reactions at various pHs were as described but with reaction buffer pH adjusted accordingly.

Primer extension analysis

Ten picomoles of unlabeled PT50 RNA were reacted under the conditions described above, except the temperature was reduced to 37 °C just prior to the addition of $MgCl_2$ and the reaction volume was 400 μL. After 1 min, the reaction was quenched with 33 mM EDTA (twice the $MgCl_2$ concentration) to a final volume of 600 μL and the RNA precipitated with ethanol. One picomole of gel-purified 5′-^{32}P-end-labeled 3′ $tRNA^{Asp}$ primer (5′-TGGCGGTCCGGACGGGAC-3′) was annealed with 1.4 pmol of reacted or unreacted (for sequencing ladders) PT50 RNA by heating to 65 °C for 2 min in buffer (50 mM Tris-HCl, pH 8.3, 15 mM NaCl, 10 mM dithiothreitol) frozen on dry ice for 2 min, and allowed to thaw on wet ice for approximately 5 min. After addition of $MgCl_2$ (6 mM in a total volume of 15 μL), five 2-μL reactions of uncleaved RNA and one of cleaved RNA were aliquoted. To four of the uncleaved reactions, 1 μL of dideoxynucleotides (either ddATP, ddCTP, ddGTP, or ddTTP) was added to a final concentration of 400 μM (to generate a sequencing ladder). The remaining uncleaved aliquot (a control for polymerase stops caused by RNA structure) and the reacted PT50 aliquot were supplemented with 1 μL of water. To all reactions, 1 μL of a dNTP mix was added to a final concentration of 5 mM. Annealed primers were extended for 5 min at 47 °C by the addition of 4 U (1 μL) of AMV reverse transcriptase (Boehringer Mannheim). Reactions were terminated by freezing on dry ice for 2 min. Samples were then thawed on wet ice, combined with 4 μL gel-loading buffer, heated to 95 °C for 2 min and set on ice. Aliquots of 2 μL were loaded onto 6% (19:1) polyacrylamide (8 M urea) gels. Gels were run approximately 1.5 h at 50 W, dried, and the bands resolved by autoradiography.

Site-specific functional group modifications

Phosphorothioate modifications at individual nucleotide positions were made from the ligation of two sets of RNA fragments to generate the corresponding PT50 and PT332(-5) self-cleaving constructs (Moore & Sharp, 1992). Specifically for PT50, phosphorothioate modifications at positions A65, A66, A67, G68, or U69 were incorporated by chemical synthesis (Dharmacon) into an 11-nt RNA fragment (5′P4GapB) corresponding to positions 63–73 of the *Escherichia coli* RNase P ribozyme. R_P or S_P phosphorothioate stereo isomers of the RNA fragments were separated by reverse phase HPLC as described by Slim and Gait (1991), and the individual stereoisomers verified by digestion with snake venom phosphodiesterase (Burgers et al., 1979). 5′P4GapB oligonucleotides were subsequently phosphorylated with T4 polynucleotide kinase (Gibco-BRL) and ATP.

Purified RNA fragments of 5′P4GapB with no modification or R_P or S_P phosphorothioate modifications as noted above were then ligated by the method of Moore and Sharp (1992) to a 5′-^{32}P-end-labeled 11-nt synthetic RNA fragment (5′P4GapA) containing positions 52–63 of *E. coli* RNase P RNA and a large RNA transcript (G73PT50, see above) containing the remainder of the PT50 ribozyme. Equal amounts (10 pmol) of 5′-^{32}P-end-labeled 5′P4GapA, 5′P4GapB,

G73PT50, and a DNA oligonucleotide (complementary to 5′P4GapA, 5′P4GapB, and the first 20 nt of G73PT50) were combined in a total volume of 6.8 μL (in distilled water), heated to 60 °C for 2 min and then immediately frozen on dry ice for at least 2 min. Samples were then thawed on wet ice and supplemented with 1 μL 10× T4 ligase buffer (New England Biolabs) 1 μL 50% 8,000 g/mol polyethylene glycol (Fluka), 0.5 μL (200 U) rRNasin (Promega) and 0.7 μL (280 U) T4 DNA ligase (New England Biolabs). Samples were then incubated for 2 h at 30 °C, combined with an equal volume (10 μL) of gel-loading buffer, heated to 90 °C for 2 min and purified on a 6% (19:1) polyacrylamide (8 M urea) gel. Ligated RNAs were visualized by autoradiography and were excised from the gel and recovered as described above.

Site-specific phosphorothioate substitution at position A352 was made in the context of four RNA fragments that gave rise to the self-cleaving conjugate PT332(-5). Three of the four RNA fragments, 3′P4GapA, 3′P4GapB, and 3′P4GapC, corresponding to nucleotides 332–343, 344–353, and 354–363, were synthesized (Dharmacon) with 3′P4GapB in the presence or absence of a phosphorothioate 5′ to position 352. Prior to ligation 3′P4GapA was 5′ ^{32}P end labeled with 150 μCi of [γ-^{32}P]-ATP (New England Nuclear) and T4 polynucleotide kinase (Gibco-BRL) and 3′P4GapB and 3′P4GapC were phosphorylated as described above. The forth fragment G364PT332, corresponding to the PT332(-5) ribozyme beginning at position 364, was produced by in vitro transcription (see above). G364PT332(-5) was hybridized along with 3′P4GapA, 3′P4GapB, and 3′P4GapC to a bridging DNA oligonucleotide complementary to positions 332–376 and ligated as described above.

ACKNOWLEDGMENTS

We are indebted to Dr. Rick Padgett for his assistance in purifying phosphorothioate stereoisomers in RNA oligonucleotides by HPLC. We also thank Frank Campbell, Dr. Mark Caprara, Adam Cassano, Dr. Jonatha Gott, Dr. Scott Strobel and Nathan Zahler for careful reading of the manuscript. This work was supported by National Institutes of Health (NIH) grant GM56740 to M.E.H. N.M.K received predoctoral training support from NIH grant GM08056.

Received January 6, 2000; returned for revision January 26, 2000; revised manuscript received January 26, 2000

REFERENCES

Altman S, Kirsebom LA. 1999. Ribonuclease P. In: Gesteland RF, Cech T, Atkins JF, eds. *The RNA world*. Cold Spring Harbor, New York: Cold Spring Harbor Laboratory Press. pp 351–380.

Basu S, Strobel SA. 1999. Thiophilic metal ion rescue of phosphorothioate interference within the *Tetrahymena* ribozyme P4-P6 domain. *RNA 5*:1399–1407.

Beebe JA, Kurz JC, Fierke CA. 1996. Magnesium ions are required by *Bacillus subtilis* ribonuclease P RNA for both binding and cleaving precursor tRNA^{Asp}. *Biochemistry 35*:10493–10505.

Brautigam CA, Steitz TA. 1998. Structural principles for the inhibition of the 3′–5′ exonuclease activity of *Escherichia coli* DNA polymerase I by phosphorothioates. *J Mol Biol 277*:363–377.

Burgers PM, Eckstein F, Hunneman DH. 1979. Stereochemistry of hydrolysis by snake venom phosphodiesterase. *J Biol Chem 254*:7476–7478.

Burgin AB, Pace NR. 1990. Mapping the active site of ribonuclease P RNA using a substrate containing a photoaffinity agent. *EMBO J 9*:4111–4118.

Cate JH, Doudna JA. 1996. Metal-binding sites in the major groove of a large ribozyme domain. *Structure 4*:1221–1229.

Cate JH, Hanna RL, Doudna JA. 1997. A magnesium ion core at the heart of a ribozyme domain. *Nature Struct Biol 4*:553–558.

Chen JL, Nolan JM, Harris ME, Pace NR. 1998. Comparative photocrosslinking analysis of the tertiary structures of *Escherichia coli* and *Bacillus subtilis* RNase P RNAs. *EMBO J 17*:1515–1525.

Chen JL, Pace NR. 1997. Identification of the universally conserved core of ribonuclease P RNA. *RNA 3*:557–560.

Chen Y, Li X, Gegenheimer P. 1997. Ribonuclease P catalysis requires Mg^{2+} coordinated to the *pro*-R_P oxygen of the scissile bond. *Biochemistry 36*:2425–2438.

Christian EL, Harris ME. 1999. The track of the pre-tRNA 5′ leader in the ribonuclease P ribozyme-substrate complex. *Biochemistry 38*:12629–12638.

Christian EL, McPheeters DS, Harris ME. 1998. Identification of individual nucleotides in the bacterial ribonuclease P ribozyme adjacent to the pre-tRNA cleavage site by short-range photocrosslinking. *Biochemistry 37*:17618–17628.

Correll CC, Freeborn B, Moore PB, Steitz TA. 1997. Metals, motifs, and recognition in the crystal structure of a 5S rRNA domain. *Cell 91*:705–712.

Eckstein F. 1985. Nucleoside phosphorothioates. *Annu Rev Biochem 54*:367–402.

Frank DN, Harris ME, Pace NR. 1994. Rational design of self-cleaving pre-tRNA ribonuclease P RNA conjugates. *Biochemistry 33*:10800–10808.

Frank DN, Pace NR. 1997. In vitro selection for altered divalent metal specificity in the RNase P RNA. *Proc Natl Acad Sci USA 94*:14355–14360.

Frank DN, Pace NR. 1998. Ribonuclease P: Unity and diversity in a tRNA processing ribozyme. *Annu Rev Biochem 67*:153–180.

Guerrier-Takada C, Gardiner K, Marsh T, Pace N, Altman S. 1983. The RNA moiety of ribonuclease P is the catalytic subunit of the enzyme. *Cell 35*:849–857.

Guerrier-Takada C, Haydock K, Allen L, Altman S. 1986. Metal ion requirements and other aspects of the reaction catalyzed by M1 RNA, the RNA subunit of ribonuclease P from *Escherichia coli*. *Biochemistry 25*:1509–1515.

Haas ES, Brown JW, Pitulle C, Pace NR. 1994. Further perspective on the catalytic core and secondary structure of ribonuclease P RNA. *Proc Natl Acad Sci USA 91*:2527–2531.

Hardt WD, Erdmann VA, Hartmann RK. 1996. R_p-deoxy-phosphorothioate modification interference experiments identify 2′-OH groups in RNase P RNA that are crucial to tRNA binding. *RNA 2*:1189–1198.

Hardt WD, Warnecke JM, Erdmann VA, Hartmann RK. 1995. R_p-phosphorothioate modifications in RNase P RNA that interfere with tRNA binding. *EMBO J 14*:2935–2944.

Harris ME, Pace NR. 1995. Identification of phosphates involved in catalysis by the ribozyme RNase P RNA. *RNA 1*:210–218.

Heide C, Pfeiffer T, Nolan JM, Hartmann RK. 1999. Guanosine 2-NH_2 groups of *Escherichia coli* RNase P RNA involved in intramolecular tertiary contacts and direct interactions with tRNA. *RNA 5*:102–116.

Kazantsev AV, Pace NR. 1998. Identification by modification-interference of purine N-7 and ribose 2′-OH groups critical for catalysis by bacterial ribonuclease P. *RNA 4*:937–947.

Kirsebom LA, Svard SG. 1994. Base pairing between *Escherichia coli* RNase P RNA and its substrate. *EMBO J 13*:4870–4876.

Knowles JR. 1980. Enzyme-catalyzed phosphoryl transfer reactions. *Annu Rev Biochem 49*:877–919.

Konforti BB, Abramovitz DL, Duarte CM, Karpeisky A, Beigelman L, Pyle AM. 1998. Ribozyme catalysis from the major groove of group II intron domain 5. *Mol Cell 1*:433–441.

Kufel J, Kirsebom LA. 1996. Different cleavage sites are aligned differently in the active site of M1 RNA, the catalytic subunit of *Escherichia coli* RNase P. *Proc Natl Acad Sci USA 93*:6085–6090.

Kufel J, Kirsebom LA. 1998. The P15-loop of *Escherichia coli* RNase P RNA is an autonomous divalent metal ion binding domain. *RNA 4*:777–788.

Kurz JC, Niranjanakumari S, Fierke CA. 1998. Protein component of

Bacillus subtilis RNase P specifically enhances the affinity for precursor-tRNA^{Asp}. *Biochemistry 37*:2393–2400.
Loria A, Pan T. 1996. Domain structure of the ribozyme from eubacterial ribonuclease P. *RNA 2*:551–563.
Loria A, Pan T. 1998. Recognition of the 5′ leader and the acceptor stem of a pre-tRNA substrate by the ribozyme from *Bacillus subtilis* RNase P. *Biochemistry 37*:10126–10133.
Massire C, Jaeger L, Westhof E. 1998. Derivation of the three-dimensional architecture of bacterial ribonuclease P RNAs from comparative sequence analysis. *J Mol Biol 279*:773–793.
Michel F, Hanna M, Green R, Bartel DP, Szostak JW. 1989. The guanosine binding site of the *Tetrahymena* ribozyme. *Nature 342*:391–395.
Moore MJ, Sharp PA. 1992. Site-specific modification of pre-mRNA: The 2′-hydroxyl groups at the splice sites. *Science 256*:992–997.
Narlikar GJ, Herschlag D. 1997. Mechanistic aspects of enzymatic catalysis: Lessons from comparison of RNA and protein enzymes. *Annu Rev Biochem 66*:19–59.
Nolan JM, Burke DH, Pace NR. 1993. Circularly permuted tRNAs as specific photoaffinity probes of ribonuclease P RNA structure. *Science 261*:762–765.
Pan T. 1995. Higher order folding and domain analysis of the ribozyme from *Bacillus subtilis* ribonuclease P. *Biochemistry 34*:902–909.
Pan T, Fang X, Sosnick T. 1999. Pathway modulation, circular permutation and rapid RNA folding under kinetic control. *J Mol Biol 286*:721–731.
Pan T, Jakacka M. 1996. Multiple substrate binding sites in the ribozyme from *Bacillus subtilis* RNase P. *EMBO J 15*:2249–2255.
Pan T, Loria A, Zhong K. 1995. Probing of tertiary interactions in RNA: 2′-hydroxyl-base contacts between the RNase P RNA and pre-tRNA. *Proc Natl Acad Sci USA 92*:12510–12514.
Pan T, Sosnick TR. 1997. Intermediates and kinetic traps in the folding of a large ribozyme revealed by circular dichroism and UV absorbance spectroscopies and activity. *Nat Struct Biol 4*:931–938.
Patel DJ. 1999. Adaptive recognition in RNA complexes with peptides and protein modules. *Curr Opin Struct Biol 9*:74–87.
Piccirilli JA, Vyle JS, Caruthers MH, Cech TR. 1993. Metal ion catalysis in the *Tetrahymena* ribozyme reaction. *Nature 361*: 85–88.
Pyle AM. 1996. Role of metal ions in ribozymes. *Metal Ions Biol Syst 32*:479–520.
Reich C, Olsen GJ, Pace B, Pace NR. 1988. Role of the protein moiety of ribonuclease P, a ribonucleoprotein enzyme. *Science 239*:178–181.
Sarkar G, Sommer SS. 1990. The “megaprimer” method of site-directed mutagenesis. *Biotechniques 8*:404–407.
Scott EC, Uhlenbeck OC. 1999. A re-investigation of the thio effect at the hammerhead cleavage site. *Nucleic Acids Res 27*:479–484.
Shan So, Yoshida A, Sun S, Piccirilli JA, Herschlag D. 1999. Three metal ions at the active site of the *Tetrahymena* group I ribozyme. *Proc Natl Acad Sci USA 96*:12299–12304.
Siew D, Zahler NH, Cassano AG, Strobel SA, Harris ME. 1999. Identification of adenosine functional groups involved in substrate binding by the ribonuclease P ribozyme. *Biochemistry 38*:1873–1883.
Slim G, Gait MJ. 1991. Configurationally defined phosphorothioate-containing ribonucleotides in the study of the mechanism of cleavage of hammerhead ribozymes. *Nucleic Acids Res 19*:1183–1188.
Smith D, Burgin AB, Haas ES, Pace NR. 1992. Influence of metal ions on the ribonuclease P reaction. Distinguishing substrate binding from catalysis. *J Biol Chem 267*:2429–2436.
Smith D, Pace NR. 1993. Multiple magnesium ions in the ribonuclease P reaction mechanism. *Biochemistry 32*:5273–5281.
Warnecke JM, Furste JP, Hardt WD, Erdmann VA, Hartmann RK. 1996. Ribonuclease P (RNase P) RNA is converted to a Cd(2+)-ribozyme by a single R_p-phosphorothioate modification in the precursor tRNA at the RNase P cleavage site. *Proc Natl Acad Sci USA 93*:8924–9828.
Weeks KM, Crothers DM. 1993. Major groove accessibility of RNA. *Science 261*:1574–1577.
Weinstein LB, Jones BC, Cosstick R, Cech TR. 1997. A second catalytic metal ion in group I ribozyme. *Nature 388*:805–808.
Yoshida A, Sun S, Piccirilli JA. 1999. A new metal ion interaction in the *Tetrahymena* ribozyme reaction revealed by double sulfur substitution. *Nat Struct Biol 6*:318–321.
Zarrinkar PP, Wang J, Williamson JR. 1996. Slow folding kinetics of RNase P RNA. *RNA 2*:564–573.